ResearchGate

See discussions, stats, and author profiles for this publication at: https://www.researchgate.net/publication/271723457

# Dynamic Coupling between Electrode Interface and Donor/Acceptor Interface via Charge Dissociation in Organic Solar Cells at Device-Operating Condition

**ARTICLE** *in* THE JOURNAL OF PHYSICAL CHEMISTRY C · JANUARY 2015

Impact Factor: 4.77 · DOI: 10.1021/acs.jpcc.5b00082

CITATION
1

READS
20

**6 AUTHORS**, INCLUDING:

Ting Wu
University of Tennessee
**13** PUBLICATIONS **29** CITATIONS
SEE PROFILE

Yu-Che Hsiao
University of Tennessee
**20** PUBLICATIONS **39** CITATIONS
SEE PROFILE

Mingxing Li
University of Tennessee
**13** PUBLICATIONS **47** CITATIONS
SEE PROFILE

Nam-Goo Kang
The University of Tennessee Knoxville
**36** PUBLICATIONS **358** CITATIONS
SEE PROFILE

Available from: Ting Wu
Retrieved on: 25 January 2016

THE JOURNAL OF PHYSICAL CHEMISTRY C

Article

pubs.acs.org/JPCC

# Dynamic Coupling between Electrode Interface and Donor/Acceptor Interface via Charge Dissociation in Organic Solar Cells at Device-Operating Condition

Ting Wu,[†] Yu-Che Hsiao,[†] Mingxing Li,[†] Nam-Goo Kang,[‡] Jimmy W. Mays,[‡] and Bin Hu*[,†]

[†]Department of Materials Science and Engineering, University of Tennessee, 1508 Middle Drive, Knoxville, Tennessee 37996, United States

[‡]Department of Chemistry, University of Tennessee, 1420 Circle Drive, Knoxville, Tennessee 37996, United States

**ABSTRACT:** Organic solar cells exhibit both electrode/photovoltaic (E/P) interface and donor/acceptor (D/A) interface in controlling the critical photovoltaic processes. Here, on the basis of the efficient PTB7:$PC_{71}BM$ solar cells, our studies on magneto-photocurrent with external bias provide the first evidence that the E/P interface and D/A interface are dynamically coupled at device-operating condition. Specifically, we observe a significant decrease (90%) in the critical bias required to completely dissociate the charge transfer (CT) states at D/A interface by changing the E/P interface with increased interface dipole field from ZnO to the polyelectrolyte (PFN). The experimental results demonstrate that strong dipole field at the E/P interface can effectively decrease the electron−hole binding energy at D/A interface through the enhancement of built-in field applied on CT states. Clearly, our experimental studies provide new insight on the interfacial engineering through addressing the dynamic coupling between E/P interface and D/A interface in organic bulk-heterojunction solar cells toward further improvement on photovoltaic efficiencies.

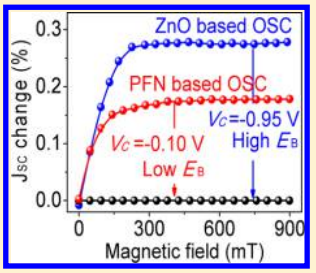


## INTRODUCTION

The materials design and interface engineering have led the power conversion efficiencies (PCEs) of polymer/fullerene heterojunction solar cells significantly improved toward 10% over the past few years.[1−7] The experimental studies have shown that both the electrode/photovoltaic (E/P) interface[8−17] and donor/acceptor (D/A) interface[18−24] play a critical role in developing high-efficiency organic solar cells (OSC). Generally, the E/P interface is accountable for the charge collection to suppress the charge accumulation in generating photocurrent. The interfacial materials at the E/P interface, including self-assembled monolayers, inorganic metal oxides, and conjugated polymers, have been well-studied due to their multiple functions, such as changing the light harvesting,[4,25] improving charge collection due to the modification of electrode work-function, enhancing the local field due to the interfacial dipoles, etc.[8−17] The D/A interface is responsible for controlling the charge dissociation, along with charge recombination toward the generation of free charge carriers. Theoretically, the dissociated charge carriers inevitably experience Coulomb attractions in the intermolecular charge-transfer (CT) states at the D/A interface,[21,22,26−28] and the dissociation of these CT states is essentially driven by local fields.[8,18] Therefore, it is intuitive to assume that the E/P interface and D/A interface are dynamically coupled through the local field in generating photovoltaic actions.

Despite the fact that the modification of the E/P interface can cause the changes in the morphological structures of the bulk D/A interfaces,[29−31] an important open question is whether these two interfaces can mutually affect each other through physical mechanisms. It is known that the electron−hole binding energy ($E_B$) of CT states at the D/A interface plays an important role in generating photocurrent in OSCs.[32−34] It is worth noting that magneto-photocurrent combined with external electric field (V-$MFE_{PC}$) can provide an estimate on $E_B$ at the D/A interface by minoring the critical voltage required to completely dissociate the CT states.[35] On the other hand, the photoinduced capacitance−voltage ($C-V$) measurement enables us to characterize the charge accumulation at the E/P interface and evaluate the built-in electric field ($E_{bi}$) under device-operating condition. Here, on the basis of the efficient PTB7:$PC_{71}BM$ solar cells, we studied two E/P interface materials, including metal oxide crystal-zinc oxide (ZnO) and water/alcohol soluble conjugated polyelectrolyte, poly[(9,9-dioctyl-2,7-fluorene)-*alt*-(9,9-bis(3′-(*N*,*N*-dimethylamino)propyl)-2,7-fluorene)] (PFN). The combination of V-$MFE_{PC}$ and $C-V$ measurements enables us to elucidate the dynamic coupling between the E/P and D/A interfaces.

## EXPERIMENTAL AND THEORETICAL METHODS

**Device Fabrication.** PTB7 and $PC_{71}BM$ (from 1-material) were blended with a weight ratio of 1:1.5 and dissolved in chlorobenzene/1,8-diiodoctane (from Sigma-Aldrich, volume ratio of 97:3) with the concentration of 25 mg/mL. Poly[(9,9-dioctyl-2,7-fluorene)-*alt*-(9,9-bis(3′-(*N*,*N*-dimethylamino)-propyl)-2,7-fluorene)] (PFN, from Ossila) was dissolved in

**Received:** January 5, 2015
**Revised:** January 11, 2015
**Published:** January 12, 2015


© 2015 American Chemical Society

DOI: 10.1021/acs.jpcc.5b00082
*J. Phys. Chem. C* 2015, 119, 2727−2732

methanol/acetic acid with the concentration of 2.5 mg/mL. The precursor solution of ZnO was prepared by sol−gel method according to the literature.[36] The inverted solar cells were fabricated with the structure of ITO/PFN or ZnO/PTB7:$PC_{71}BM$/$MoO_3$/Ag. The layer of PFN and ZnO was spin-coated on top of ITO (indium−tin−oxide) with thicknesses of 12 and 30 nm, respectively. The active layer with a thickness of 90 nm was prepared by spin coating and followed by the thermal deposition of 10 nm $MoO_3$ and 100 nm silver under the vacuum of $2 \times 10^{-6}$ Torr. All processes were taken inside the glovebox with both moisture and oxygen below 1 ppm.

**Characterization.** Photovoltaic parameters were determined from the current−voltage characteristics by using Keithley 2400 source meter under photoexcitation of AM 1.5G 100 mW $cm^{-2}$ from Thermal Oriel 96000 300 W solar simulator. The magneto-photocurrent ($MFE_{PC}$) was measured under photoexcitation of 532 nm CW laser beam (25 mW/$cm^2$), which was perpendicularly incident on the active area from the transparent ITO-electrode side; the magnetic field was applied parallel to the device plane, suggesting that the magnetic field was perpendicular to the built-in field. It is worth noting that the $MFE_{PC}$ does not show appreciable angle dependence with magnetic field direction. The amplitude of photocurrent change ($MFE_{PC}$ (%)) is determined by the relative change in photocurrent at short-circuit conditions:

$$MFE_{PC}(\%) = [I_{CT(B)} - I_{CT(0)}]/[I + I_{CT(0)}] \quad (1)$$

Here the $I$ and $I_{CT}$ are the photocurrents generated through non-CT states (or excitons) and CT states, which are insensitive and sensitive to the applied magnetic field due to the relative large and small spin-exchange energies, respectively.[37] $I_{(B)}$ and $I_{(0)}$ are short-circuit currents with and without applied magnetic field, respectively. The external reverse bias was applied by Keithley 2400 source meter. The characterization of remnant polarization was carried out by using ferroelectric test systems (RADIANT Technologies. Inc.) with the hysteresis period of 50 ms, preset delay of 1000 ms, and maximum voltage of 100 mV. Photoinduced capacitance−voltage characteristics were measured under an alternating voltage of 50 mV at 1 kHz by dielectric spectrometer (Agilent, E4980A). The light illumination intensity was changed by using different neutral optical filters.

## RESULTS AND DISCUSSION

As illustrated in Figure 1a, decent devices can be conveniently obtained by combining PTB7/$PC_{71}BM$ inverted design with appropriate E/P interface (ZnO and PFN). Particularly, the PFN based E/P interface gives an enhancement of 37% in PCE as compared to the ZnO based E/P interface.

On the basis of the above two systems, we performed the measurement of magneto-photocurrent combined with external electric field (V-$MFE_{PC}$). The results shown in Figure 1b,c turn out three interesting phenomena. First, the magneto-photocurrent ($MFE_{PC}$) signal indicates the formation of intermolecular CT states at D/A interface in PTB7:$PC_{71}BM$ inverted solar cells. It is known that the CT states can be formed with both singlet ($CT^1$) and triplet ($CT^3$) configurations at the D/A interface under photoexcitation due to electron spin multiplicities.[38,39] An external magnetic field can change the singlet/triplet ratios during the formation of CT states through spin-dependent recombination[40,41] due to field gradient effects[42] in

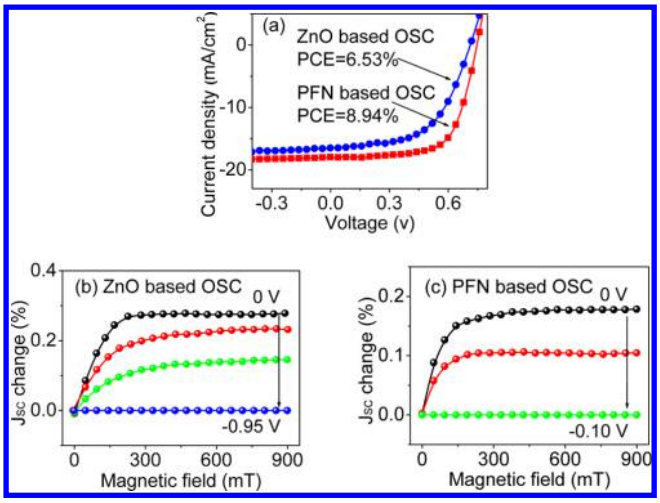


**Figure 1.** Current−voltage characteristics for the inverted PTB7/$PC_{71}BM$ solar cells with the ZnO and PFN based E/P interfaces (a) Magneto-photocurrent with external reverse bias for the inverted PTB7:$PC_{71}BM$ solar cells with the ZnO (b) and PFN (c) based E/P interface, respectively.

spin precessions or after the formation of CT states through perturbing the intersystem crossing (ISC).[43−45] Consequently, changing the singlet/triplet ratios can cause a change in the photocurrent since $CT^1$ has a higher dissociation rate due to more a ionic nature in the wave function as compared to that of $CT^3$.[46−48] It is clear that both of the two devices present positive $MFE_{PC}$, suggesting that the short circuit current (Jsc) increases with the magnetic field. The positive MFEpc implies that a magnetic field can increase the singlet/triplet branching ratio in CT states. Here, the $MFE_{PC}$ is observed with different amplitudes: 0.3% for ZnO-based device and 0.18% for PFN-based device. From the definition of $MFE_{PC}$ amplitude (eq 1), we can see that the $MFE_{PC}$ amplitude can be essentially determined by (i) the density of CT states and (ii) magnetic field-dependent singlet/triplet branching ratio in CT states. The density of CT states is determined by the charge recombination at D/A interfaces upon exciton dissociation. In general, the charge recombination can undergo germinate and nongerminate processes to form both singlet and triplet states. Applying a magnetic field can then change the singlet/triplet branching ratio by influencing the either spin precessions during charge recombination or intersystem crossing after charge recombination. The experimental studies have shown that a magnetic field can appreciably change the singlet/triplet branching ratio in CT states.[43,49,50] This is because a magnetic field can compete with spin-exchange interactions in CT states during charge recombination or through spin conserving and mixing processes.[37,51] Clearly, monitoring the $MFE_{PC}$ signal can indicate the dissociation of CT states at D:A interfaces in organic solar cells.[33,37,43,52] We should note that the critical bias ($V_C$) required to completely quench the $MFE_{PC}$ signal is largely reduced when the E/P interface is changed from ZnO to PFN. The $V_C$ values for the ZnO based and PFN based devices are determined to be −0.95 and −0.10 V, respectively. This means that changing the E/P interface can largely change the critical bias required to completely dissociate the CT states at the D/A interface. The reduction on the $V_C$ indicates that the PFN based E/P interface leads to a stronger $E_{bi}$ to dissociate the CT states at the D/A interface. It is known that the dissociation of CT states is essentially determined by electron−hole binding


DOI: 10.1021/acs.jpcc.5b00082
J. Phys. Chem. C 2015, 119, 2727−2732

energy ($E_B$). In general, the binding energy $E_B$ at the D/A interface is controlled by two energy parameters: (i) potential energy due to Coulomb attraction and (ii) kinetic energy due to electrical drifting driven by $E_{bi}$.[33] Clearly, when $E_{bi}$ is changed, the binding energy $E_B$ at the D/A interface can be altered through electric drifting, consequently changing the generation of photocurrent in organic solar cells. Therefore, we can conclude that the modification on the E/P interface can affect the electron−hole $E_B$ at the D/A interface under device-operating conditions. Clearly, our V-MFE$_{PC}$ studies provide the first experimental evidence that the E/P and D/A interfaces are dynamically coupled during the generation of photocurrent at device-operating condition.

The early studies have shown that changing the E/P interface can affect interfacial dipole field and bulk morphologies, consequently influencing the device efficiencies.[8−14,29−31] Considering these variations, the effective built-in electric field ($E_{bi}$) can be given by eq 2.

$$E_{bi} = E'_{bi} + E_{int} - \delta \quad (2)$$

Here $E'_{bi}$ is the primary built-in electric field without considering interface variations; $E_{int}$ is the interfacial dipole field, and $\delta$ is a correction term due to charge accumulation at E/P interface. Theoretically, all the changes at the E/P interface can modify $E_{bi}$ applied onto the CT states at the D/A interface under device-operating conditions. Therefore, the D/A interface and E/P interface can become dynamic parameters in the generation of photocurrent and photovoltage at device-operating conditions in organic solar cells, schematically shown in Figure 2a.

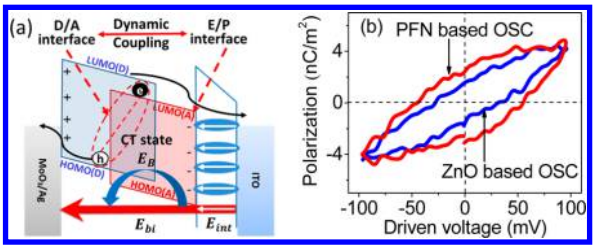


**Figure 2.** (a) Schematic diagram of dynamic coupling between electrode/photovoltaic (E/P) interface and donor/acceptor (D/A) interface at device-operating conditions through tuning the built-in field ($E_{bi}$) applied on the charge transfer (CT) states. $E_B$ and $E_{int}$ are electron−hole binding energy and interfacial dipole field, respectively. (b) Hysteresis loops of polarization as a function of driven voltage in dark conditions for the inverted PTB7:PC$_{71}$BM solar cells with the ZnO and PFN based E/P interface.

Our previous studies on the $C-V$ characteristics have shown that the PFN thin film can generate a stronger surface polarization than the ZnO.[12] Here, we characterized the ferroelectric polarization in the inverted PTB7:PC$_{71}$BM solar cells with the ZnO based and the PFN based E/P interfaces in dark conditions. As illustrated in Figure 2b, the remnant polarizations, defined as the intercept of the hysteresis loop with the polarization axis,[53−55] are given at 1.52 and 3.08 nC/m$^2$ for the ZnO and PFN based devices. We can see that using the PFN based E/P interface can largely increase the remnant polarization, as compared to the ZnO based E/P interface, in the inverted PTB7:PC$_{71}$BM solar cells. This phenomenon suggests that the PFN and ZnO based E/P interfaces give stronger and weaker interfacial polarizations in the inverted PTB7:PC$_{71}$BM solar cells, respectively. It is noted that the surface polarization can generate an interfacial dipole field in the same direction as the built-in field $E_{bi}$, as shown in eq 2, to enhance the dissociation of CT states.

Furthermore, Figure 3a,b shows the $C-V$ spectra at different photoexcitation intensities for PTB7:PC$_{71}$BM inverted solar

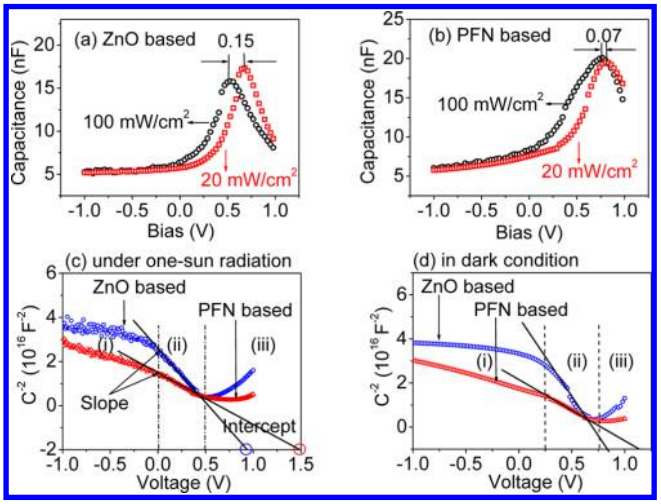


**Figure 3.** Photoinduced capacitance−voltage ($C-V$) characteristics for the inverted PTB7:PC$_{71}$BM solar cells with the ZnO based E/P interface (a) and the PFN based E/P interface (b). Measurements were taken under the photoexcitation intensities of 100 mW/cm$^2$ (○) and 20 mW/cm$^2$ (□), respectively. $C^{2-}-V$ characteristics under one sun radiation (c) and in dark conditions (d): i, ii, and iii represent neutral region, space charge region, and recombination region, respectively.

cells with the ZnO based and PFN based E/P interfaces, respectively. We can see that increasing photoexcitation intensity can cause a shift on the peak voltage ($V_{peak}$) in the $C-V$ spectrum. This $V_{peak}$ shift can essentially reflect the charge accumulation at the E/P interface.[10,56] Large and small $V_{peak}$ shifts correspond to high and low charge accumulation at the E/P interface, respectively. Therefore, we can conclude that the device with PFN based E/P interface has less charge accumulation than that with ZnO based E/P interface. Clearly, increasing the surface polarization at the E/P interface can decrease the charge accumulation at respective electrodes. This can consequently increase $E_{bi}$ due to small value of $\delta$, as shown in eq 2, in organic solar cells under device-operating condition.

On the basis of the $C-V$ spectra, we applied the classical Mott−Schottky relation (eqs 3 and 4)[57,58] to evaluate $E_{bi}$ based on $C^{2-}-V$ characteristics under the one sun radiation and in the dark conditions.

$$C^{-2} = \frac{2(V_{bi} - V)}{A^2 e \varepsilon \varepsilon_0 N_A} \quad (3)$$

$$V_{bi} = \frac{\text{intercept}}{|\text{slope}|} \quad (4)$$

Here, $C$ represents the capacitance, $V_{bi}$ is the built-in potential, $V$ is the applied bias, $A$ is the active area, $e$ is the elementary charge of electron, $\varepsilon_r$ is the relative dielectric constant of the medium, and $\varepsilon_0$ is the permittivity of vacuum. $N_A$ is the density of excited states.

As shown in Figure 3c,d, the $C^{2-}-V$ characteristics can be divided into three regions related to neutral state, space charges, and charge recombination. Here, the intercept of the


DOI: 10.1021/acs.jpcc.5b00082
J. Phys. Chem. C 2015, 119, 2727−2732

Table 1. Effective Built-In Potential ($V_{bi}$) for the Inverted PTB7:$PC_{71}BM$ Solar Cells with the ZnO and PFN Based E/P Interface under One Sun Radiation and in Dark Conditions, Respectively

| | one sun photoexcitation | | | dark condition | | |
|---|---|---|---|---|---|---|
| interlayer | intercept ($\times 10^{16}$) | slope ($\times 10^{16}$) | $V_{bi}$ (V) | intercept ($\times 10^{16}$) | slope ($\times 10^{16}$) | $V_{bi}$ (V) |
| ZnO | 2.56 | −4.51 | 0.55 | 4.33 | −6.02 | 0.72 |
| PFN | 1.39 | −1.86 | 0.75 | 2.09 | −2.63 | 0.79 |

tangent of the $C^{2-}-V$ curve in the space charge region can be used to evaluate $E_{bi}$. Table 1 summarizes the following two points. First, increasing the interfacial dipole fields by changing the E/P interface from ZnO to PFN leads to an increment of 36% and 10% on $E_{bi}$ under the one sun radiation and in the dark conditions, respectively. This indicates that the difference in surface polarization between the PFN and ZnO based E/P interfaces becomes larger under photoexcitation condition as compared to dark condition. Second, a more remarkable decrease in $E_{bi}$ from dark condition to one sun radiation is observed in the ZnO based device relative to the PFN based device. Upon combination with the charge accumulation results related to PFN and ZnO based E/P interfaces shown in Figure 3a,b, we can confirm that the surface accumulation of photogenerated charge carriers can affect the built-in electric field $E_{bi}$. A greater surface accumulation of photogenerated charge carriers corresponds to a lower $E_{bi}$.

## CONCLUSION

In summary, our V-$MFE_{PC}$ studies provide the first experimental evidence that the E/P interface and D/A interface are dynamically coupled through local field during charge dissociation, accumulation, and recombination processes in the organic bulk-heterojunction solar cells at device-operating conditions. In particular, we observed large decreases in both the signal magnitude and the critical bias required to completely dissociate the CT states at the D/A interface when the E/P interface is changed from ZnO to PFN. The experimental results indicate that the built-in electric field applied onto the CT states is enhanced by replacing ZnO with PFN. This can increase the charge dissociation at the D/A interface, leading to a decrease in the electron−hole binding energy. The results of ferroelectric polarization measurement reveal that the polyelectrolyte-PFN can generate stronger interface polarization at E/P interface as compared to ZnO. The increase in the interface polarization not only enhances the interfacial dipole fields, but also increases the charge dissociation at D/A interface through built-in field. The photoinduced $C-V$ characteristics show that the built-in electric field is enhanced by 36% and 10% under one sun photoexcitation and dark conditions, respectively, when replacing ZnO by PFN. Clearly, our experimental studies present new insight on the dynamic coupling between E/P interface and D/A interface in organic solar cells at device-operating condition for the further improvement on the photovoltaic efficiencies.

## AUTHOR INFORMATION

### Corresponding Author

*E-mail: bhu@utk.edu.

### Author Contributions

B.H. directed the research project. T.W. designed and performed the experiments and analyzed the data. T.W. and B.H. cowrote the manuscript. Y.-C.H., N.-G.K., and J.W.M. made contributions to the discussion of the manuscript.

### Notes

The authors declare no competing financial interest.

## ACKNOWLEDGMENTS

This research was supported by the financial support from Air Force Office of Scientific Research (AFOSR) under Grant FA9550-11-1-0082 and National Science Foundation (ECCS-1102011 and CBET-1438181). The authors also acknowledge the support from Sustainable Energy Education and Research Center and Center for Materials Processing at the University of Tennessee. This research was partially conducted at the Center for Nanophase Materials Sciences based on user project (CNMS2012-106, CNMS2012-107, CNMS-2012-108), which is sponsored at Oak Ridge National Laboratory by the Division of Scientific User Facilities, U.S. Department of Energy. The authors at the University of Tennessee also acknowledge the project support from National Science Foundation of China (Grants 21161160445 and 61077020). N.G.K. and J.W.M. acknowledge support by the Materials Science and Engineering Division, U.S. Department of Energy (DoE), Office of Basic Energy Sciences (BES) under Contract No. DEAC05-00OR22725 with UT-Battelle, LLC at Oak Ridge National Laboratory (ORNL).

## REFERENCES

(1) Park, S. H.; Roy, A.; Beaupré, S.; Cho, S.; Coates, N.; Moon, J. S.; Moses, D.; Leclerc, M.; Lee, K.; Heeger, A. J. Bulk Heterojunction Solar Cells with Internal Quantum Efficiency Approaching 100%. *Nat. Photonics* **2009**, *3*, 297−302.

(2) Zhao, G.; He, Y.; Li, Y. 6.5% Efficiency of Polymer Solar Cells based on Poly(3-hexylthiophene) and Indene-C(60) Bisadduct by Device Optimization. *Adv. Mater.* **2010**, *22*, 4355−4358.

(3) Su, M. S.; Kuo, C. Y.; Yuan, M. C.; Jeng, U. S.; Su, C. J.; Wei, K. H. Improving Device Efficiency of Polymer/Fullerene Bulk Heterojunction Solar Cells through Enhanced Crystallinity and Reduced Grain Boundaries Induced by Solvent Additives. *Adv. Mater.* **2011**, *23*, 3315−3319.

(4) He, Z.; Zhong, C.; Su, S.; Xu, M.; Wu, H.; Cao, Y. Enhanced Power-Conversion Efficiency in Polymer Solar Cells Using An Inverted Device Structure. *Nat. Photonics* **2012**, *6*, 591−595.

(5) You, J.; Dou, L.; Yoshimura, K.; Kato, T.; Ohya, K.; Moriarty, T.; Emery, K.; Chen, C. C.; Gao, J.; Li, G.; et al. A Polymer Tandem Solar Cell with 10.6% Power Conversion Efficiency. *Nat. Commun.* **2013**, *4*, 1446.

(6) Lu, L.; Yu, L. Understanding Low Bandgap Polymer PTB7 and Optimizing Polymer Solar Cells Based on It. *Adv. Mater.* **2014**, *26*, 4413−4430.

(7) Lu, L.; Xu, T.; Chen, W.; Landry, E. S.; Yu, L. Ternary Blend Polymer Solar Cells with Enhanced Power Conversion Efficiency. *Nat. Photonics* **2014**, *8*, 716−722.

(8) Khodabakhsh, S.; Sanderson, B. M.; Nelson, J.; Jones, T. S. Using Self-Assembling Dipole Molecules to Improve Charge Collection in Molecular Solar Cells. *Adv. Funct. Mater.* **2006**, *16*, 95−100.

(9) Greiner, M. T.; Chai, L.; Helander, M. G.; Tang, W.-M.; Lu, Z.-H. Metal/Metal-Oxide Interfaces: How Metal Contacts Affect the



DOI: 10.1021/acs.jpcc.5b00082
J. Phys. Chem. C 2015, 119, 2727−2732

Work Function and Band Structure of $MoO_3$. *Adv. Funct. Mater.* **2013**, *23*, 215−226.
(10) Boix, P. P.; Ajuria, J.; Etxebarria, I.; Pacios, R.; Garcia-Belmonte, G.; Bisquert, J. Role of ZnO Electron-Selective Layers in Regular and Inverted Bulk Heterojunction Solar Cells. *J. Phys. Chem. Lett.* **2011**, *2*, 407−411.
(11) He, Z.; Zhong, C.; Huang, X.; Wong, W.-Y.; Wu, H.; Chen, L.; Su, S.; Cao, Y. Simultaneous Enhancement of Open-Circuit Voltage, Short-Circuit Current Density, and Fill Factor in Polymer Solar Cells. *Adv. Mater.* **2011**, *23*, 4636−4643.
(12) Hsiao, Y.-C.; Zang, H.; Ivanov, I.; Xu, T.; Lu, L.; Yu, L.; Hu, B. Dielectric Interface Effects on Surface Charge Accumulation and Collection towards High-Efficiency Organic Solar Cells. *J. Appl. Phys.* **2014**, *115*, 154506.
(13) Yuan, Y.; Reece, T. J.; Sharma, P.; Poddar, S.; Ducharme, S.; Gruverman, A.; Yang, Y.; Huang, J. Efficiency Enhancement in Organic Solar Cells with Ferroelectric Polymers. *Nat. Mater.* **2011**, *10*, 296−302.
(14) Yip, H.-L.; Jen, A. K. Y. Recent Advances in Solution-Processed Interfacial Materials for Efficient and Stable Polymer Solar Cells. *Energy Environ. Sci.* **2012**, *5*, 5994−6011.
(15) Huang, J.; Xu, Z.; Yang, Y. Low-Work-Function Surface Formed by Solution-Processed and Thermally Deposited Nanoscale Layers of Cesium Carbonate. *Adv. Funct. Mater.* **2007**, *17*, 1966−1973.
(16) Prada, S.; Martinez, U.; Pacchioni, G. Work Function Changes Induced by Deposition of Ultrathin Dielectric Films on Metals: A Theoretical Analysis. *Phys. Rev. B* **2008**, *78*, 235423.
(17) Salim, T.; Yin, Z.; Sun, S.; Huang, X.; Zhang, H.; Lam, Y. M. Solution-Processed Nanocrystalline $TiO_2$ Buffer Layer Used for Improving the Performance of Organic Photovoltaics. *ACS Appl. Mater. Interfaces* **2011**, *3*, 1063−1067.
(18) Gunes, S.; Neugebauer, H.; Sariciftci, N. S. Conjugated Olymer-Based Organic Solar Cells. *Chem. Rev.* **2007**, *107*, 1324−1338.
(19) Deibel, C.; Strobel, T.; Dyakonov, V. Role of the Charge Transfer State in Organic Donor−Acceptor Solar Cells. *Adv. Mater.* **2010**, *22*, 4097−4111.
(20) Thompson, B. C.; Frechet, J. M. Polymer-Fullerene Composite Solar Cells. *Angew. Chem., Int. Ed.* **2008**, *47*, 58−77.
(21) Zhou, Y.; Tvingstedt, K.; Zhang, F.; Du, C.; Ni, W.-X.; Andersson, M. R.; Inganäs, O. Observation of a Charge Transfer State in Low-Bandgap Polymer/Fullerene Blend Systems by Photoluminescence and Electroluminescence Studies. *Adv. Funct. Mater.* **2009**, *19*, 3293−3299.
(22) Tvingstedt, K.; Vandewal, K.; Gadisa, A.; Zhang, F.; Manca, J.; Inganas, O. Electroluminescence from charge transfer states in polymer solar cells. *J. Am. Chem. Soc.* **2009**, *131*, 11819−24.
(23) Chen, H.; Hu, S.; Zang, H.; Hu, B.; Dadmun, M. Precise Structural Development and its Correlation to Function in Conjugated Polymer: Fullerene Thin Films by Controlled Solvent Annealing. *Adv. Funct. Mater.* **2013**, *23*, 1701−1710.
(24) Chen, H.; Peet, J.; Hu, S.; Azoulay, J.; Bazan, G.; Dadmun, M. The Role of Fullerene Mixing Behavior in the Performance of Organic Photovoltaics: PCBM in Low-Bandgap Polymers. *Adv. Funct. Mater.* **2014**, *24*, 140−150.
(25) Kim, J. Y.; Kim, S. H.; Lee, H. H.; Lee, K.; Ma, W.; Gong, X.; Heeger, A. J. New Architecture for High-Efficiency Polymer Photovoltaic Cells Using Solution-Based Titanium Oxide as an Optical Spacer. *Adv. Mater.* **2006**, *18*, 572−576.
(26) Westenhoff, S.; Howard, I. A.; Friend, R. H. Probing the Morphology and Energy Landscape of Blends of Conjugated Polymers with Sub-10 nm Resolution. *Phys. Rev. Lett.* **2008**, *101*, 016102.
(27) Clarke, T. M.; Durrant, J. R. Charge Photogeneration in Organic Solar Cells. *Chem. Rev.* **2010**, *110*, 6736−6767.
(28) Bakulin, A. A.; Rao, A.; Pavelyev, V. G.; van Loosdrecht, P. H.; Pshenichnikov, M. S.; Niedzialek, D.; Cornil, J.; Beljonne, D.; Friend, R. H. The Role of Driving Energy and Delocalized States for Charge Separation in Organic Semiconductors. *Science* **2012**, *335*, 1340−1344.
(29) Campoy-Quiles, M.; Ferenczi, T.; Agostinelli, T.; Etchegoin, P. G.; Kim, Y.; Anthopoulos, T. D.; Stavrinou, P. N.; Bradley, D. D.; Nelson, J. Morphology Evolution *via* Self-Organization and Lateral and Vertical Diffusion in Polymer:Fullerene Solar Cell Blends. *Nat. Mater.* **2008**, *7*, 158−164.
(30) Park, L. Y.; Munro, A. M.; Ginger, D. S. Controlling Film Morphology in Conjugated Polymer:Fullerene Blends with Surface Patterning. *J. Am. Chem. Soc.* **2008**, *130*, 15916−15926.
(31) Bulliard, X.; Ihn, S.-G.; Yun, S.; Kim, Y.; Choi, D.; Choi, J.-Y.; Kim, M.; Sim, M.; Park, J.-H.; Choi, W.; et al. Enhanced Performance in Polymer Solar Cells by Surface Energy Control. *Adv. Funct. Mater.* **2010**, *20*, 4381−4387.
(32) Morteani, A.; Sreearunothai, P.; Herz, L.; Friend, R.; Silva, C. Exciton Regeneration at Polymeric Semiconductor Heterojunctions. *Phys. Rev. Lett.* **2004**, *92*, 247402.
(33) Zang, H.; Xu, Z.; Hu, B. Magneto-Optical Investigations on the Formation and Dissociation of Intermolecular Charge-Transfer Complexes at Donor-Acceptor Interfaces in Bulk-Heterojunction Organic Solar Cells. *J. Phys. Chem. B* **2010**, *114*, 5704−5709.
(34) Gélinas, S.; Paré-Labrosse, O.; Brosseau, C.-N.; Albert-Seifried, S.; McNeill, C. R.; Kirov, K. R.; Howard, I. A.; Leonelli, R.; Friend, R. H.; Silva, C. The Binding Energy of Charge-Transfer Excitons Localized at Polymeric Semiconductor Heterojunctions. *J. Phys. Chem. C* **2011**, *115*, 7114−7119.
(35) Zang, H.; Liang, Y.; Yu, L.; Hu, B. Intra-Molecular Donor-Acceptor Interaction Effects on Charge Dissociation, Charge Transport, and Charge Collection in Bulk-Heterojunction Organic Solar Cells. *Adv. Energy Mater.* **2011**, *1*, 923−929.
(36) Hsieh, S.-N.; Hsiao, S.-W.; Chen, T.-Y.; Li, C.-Y.; Lee, C.-H.; Guo, T.-F.; Hsu, Y.-J.; Lin, T.-L.; Wei, Y.; Wen, T.-C. Self-Assembled Tetraoctylammonium Bromide as an Electron-Injection Layer for Cathode-Independent High-Efficiency Polymer Light-Emitting Diodes. *J. Mater. Chem.* **2011**, *21*, 8715−8720.
(37) Li, M.; Wang, H.; He, L.; Zang, H.; Xu, H.; Hu, B. Optically tunable spin-exchange energy at donor:acceptor interfaces in organic solar cells. *Appl. Phys. Lett.* **2014**, *105*, 023302.
(38) Knapp, E.-W.; Schulten, K. Magnetic Field Effect on the Hyperfine-Induced Electron Spin Motion in Radicals Undergoing Diamagnetic−Paramagnetic Exchange. *J. Chem. Phys.* **1979**, *71*, 1878−1883.
(39) Musewald, C.; Gilch, P.; Hartwich, G.; Pöllinger-Dammer, F.; Scheer, H.; Michel-Beyerle, M. E. Magnetic Field Dependence of Ultrafast Intersystem-Crossing: A Triplet Mechanism on the Picosecond Time Scale? *J. Am. Chem. Soc.* **1999**, *121*, 8876−8881.
(40) Heberle, A. P.; Haacke, S.; Oestreich, M.; Potemski, M.; Ruhle, W. W.; Maan, J. C.; Kohler, K.; Weimann, G.; Queisser, H. J. Time-Resolved Luminescence of Semiconductor Heterostructures in High Magnetic-Fields. *Physica B* **1995**, *204*, 332−338.
(41) Reufer, M.; Walter, M. J.; Lagoudakis, P. G.; Hummel, A. B.; Kolb, J. S.; Roskos, H. G.; Scherf, U.; Lupton, J. M. Spin-Conserving Carrier Recombination in Conjugated Polymers. *Nat. Mater.* **2005**, *4*, 340−346.
(42) Macia, F.; Wang, F.; Harmon, N. J.; Kent, A. D.; Wohlgenannt, M.; Flatte, M. E. Organic magnetoelectroluminescence for room temperature transduction between magnetic and optical information. *Nat. Commun.* **2014**, *5*, 3609−3616.
(43) Xu, Z.; Hu, B. Photovoltaic Processes of Singlet and Triplet Excited States in Organic Solar Cells. *Adv. Funct. Mater.* **2008**, *18*, 2611−2617.
(44) Yan, L.; Shao, M.; Graeff, C. F. O.; Hummelgen, I.; Ma, D. M.; Hu, B. Changing Inter-Molecular Spin-Orbital Coupling for Generating Magnetic Field Effects in Phosphorescent Organic Semiconductors. *Appl. Phys. Lett.* **2012**, *100*, 013301.
(45) Turro, N. J.; Kraeutler, B. Magnetic field and magnetic isotope effects in organic photochemical reactions. A novel probe of reaction mechanisms and a method for enrichment of magnetic isotopes. *Acc. Chem. Res.* **1980**, *13*, 369−377.
(46) Wohlgenannt, M.; Tandon, K.; Mazumdar, S.; Ramasesha, S.; Vardeny, Z. V. Formation cross-sections of singlet and triplet excitons in [pi]-conjugated polymers. *Nature* **2001**, *409*, 494−497.


DOI: 10.1021/acs.jpcc.5b00082
*J. Phys. Chem. C* 2015, 119, 2727−2732

(47) Kalinowski, J.; Szmytkowski, J.; Stampor, W. Magnetic hyperfine modulation of charge photogeneration in solid films of $Alq_3$. *Chem. Phys. Lett.* **2003**, *378*, 380−387.
(48) Wohlgenannt, M.; Vardeny, Z. V. Spin-Dependent Exciton Formation Rates in Conjugated Materials. *J. Phys.: Condens. Matter* **2003**, *15*, R83−R107.
(49) Brocklehurst, B.; Dixon, R. S.; Gardy, E. M.; Lopata, V. J.; Quinn, M. J.; Singh, A.; Sargent, F. P. The effect of a magnetic field on the singlet/triplet ratio in geminate ion recombination. *Chem. Phys. Lett.* **1974**, *28*, 361−363.
(50) Zang, H.; Yan, L.; Li, M.; He, L.; Gai, Z.; Ivanov, I.; Wang, M.; Chiang, L.; Urbas, A.; Hu, B. Magneto-dielectric effects induced by optically-generated intermolecular charge-transfer states in organic semiconducting materials. *Sci. Rep.* **2013**, *3*, 2812.
(51) He, L.; Li, M.; Urbas, A.; Hu, B. Magnetophotoluminescence line-shape narrowing through interactions between excited states in organic semiconducting materials. *Phys. Rev. B* **2014**, *89*, 155304.
(52) Hu, B.; Yan, L.; Shao, M. Magnetic-Field Effects in Organic Semiconducting Materials and Devices. *Adv. Mater.* **2009**, *21*, 1500−1516.
(53) Hadziioannou, G.; Stein, R. S. Neutron Scattering Studies of Dimensions and of Interactions between Components in Polystyrene/Poly(vinyl methyl ether) and Poly(vinylidene fluoride)/Poly(methyl methacrylate) Amorphous Blends. *Macromolecules* **1984**, *17*, 567−573.
(54) Jo, W. H.; Yoon, J. T.; Lee, S. C. Miscibility of Poly(vinylidene fluoride) and Poly(styrene-co-methyl methacrylate) Blends. *Polym. J.* **1991**, *23*, 1243−1247.
(55) Nalwa, H. S. *Ferroelectric Polymers: Chemistry, Physics, and Applications*; Marcel Dekker Inc.: New York, 1995.
(56) Zhao, C.; Qiao, X.; Chen, B.; Hu, B. Thermal Annealing Effect on Internal Electrical Polarization in Organic Solar Cells. *Org. Electron.* **2013**, *14*, 2192−2197.
(57) Perrier, G.; de Bettignies, R.; Berson, S.; Lemaître, N.; Guillerez, S. Impedance Spectrometry of Optimized Standard and Inverted P3HT-PCBM Organic Solar Cells. *Sol. Energy Mater. Sol. Cells* **2012**, *101*, 210−216.
(58) Fabregat-Santiago, F.; Garcia-Belmonte, G.; Bisquert, J.; Bogdanoff, P.; Zaban, A. Mott-Schottky Analysis of Nanoporous Semiconductor Electrodes in Dielectric State Deposited on $SnO_2$(F) Conducting Substrates. *J. Electrochem. Soc.* **2003**, *150*, E293.


DOI: 10.1021/acs.jpcc.5b00082
*J. Phys. Chem. C* 2015, 119, 2727−2732